31. Tsai CC, Hung SC. Functional roles of pluripotency transcription factors in mesenchymal stem cells. Cell Cycle. 2012; 11:3711–2.
32. O'Donnell L. Risk of bovine spongiform encephalopathy (BSE) in collagenase enzymes. ISCT Telegraft. 2007;14:14–5.
33. Crook JM, Peura TT, Kravets L, Bosman AG, Buzzard JJ, Horne R, et al. The generation of six clinical-grade human embryonic stem cell lines. Cell Stem Cell. 2007;1:490–4.
34. Van der Laan JW, Brightwell J, McAnulty P, Ratky J, Stark C, et al. Regulatory acceptability of the minipig in the development of pharmaceuticals, chemicals, and other products. J Pharmacol Toxicol Methods. 2010;62:184–95.
35. Shimomura K, Ando W, Tateishi K, Nansai R, Fujie H, Hart DA, et al. The influence of skeletal maturity on allogenic synovial mesenchymal stem cell-based repair of cartilage in a large animal. Biomaterials. 2010;31:8004–11.
36. Moriguchi Y, Tateishi K, Ando W, Shimomura K, Yonetani Y, Tanaka Y, et al. Repair of meniscal lesions using a scaffold-free tissue-engineered construct derived from allogenic synovial MSCs in a miniature swine model. Biomaterials. 2013;34:2185–93.
37. Sachs DA, Sykes M, Yamada K. Achieving tolerance in pig-to-primate xenotransplantation: reality of fantasy. Transplantation Immunol. 2009;21:101–5.

Knee Surg Sports Traumatol Arthrosc (2015) 23:1153–1160
DOI 10.1007/s00167-014-2931-7

KNEE

Analysis of displacement and deformation of the medial meniscus with a horizontal tear using a three-dimensional computer model

Hiroshi Amano · Takehiko Iwahashi · Tomoyuki Suzuki · Tatsuo Mae · Norimasa Nakamura · Kazuomi Sugamoto · Konsei Shino · Hideki Yoshikawa · Ken Nakata

Received: 31 January 2013 / Accepted: 4 March 2014 / Published online: 15 March 2014

Abstract

Purpose The displacement and deformation of the knee meniscus significantly affect its roles; however, little is known about the displacement and deformation patterns of a torn medial meniscus. The objective of this study was to evaluate quantitatively the patterns of displacement and deformation in horizontally torn medial menisci during knee flexion.

Methods Twenty patients with horizontally torn medial menisci underwent three-dimensional (3-D) magnetic resonance imaging at varying degrees of knee flexion, and 3-D computer models of the tibia, tibial articular cartilage, and meniscus were generated. Based on these, the size of the horizontal tear (% tear) was evaluated and defined as the circumferential ratio between the length of the horizontal tear and that of the entire meniscus. The 3-D meniscus models were automatically superimposed over images taken at 0, 20, 40, and 60° of knee flexion by the voxel-based registration method. Meniscal motion and deformation during knee flexion were visualized and quantitatively calculated on the mid-sagittal plane. Correlations between the size of horizontal tear, displacement/deformation of torn menisci, and clinical symptoms were evaluated after conservative treatment for 3 months.

Results The % tear was 35.7 ± 12.5 % (range 13.7–55.5 %). During knee flexion, all torn menisci moved posteriorly, with gradual widening of horizontal and vertical gaps ($p < 0.05$). A direct correlation was observed between % tear and change in the vertical tear gap during knee flexion ($p < 0.05$). There was an inverse correlation between Lysholm score and % tear ($p < 0.05$).

Conclusion Medial meniscal horizontal tears widen and deform during knee flexion, and % tear correlates with the change in the vertical gap. Patients with a lower % tear are more capable of performing activities of daily living after conservative treatment. This method may help clarify the cause of pain in patients with medial meniscus tears as well as facilitate the selection of an appropriate treatment plan.

Level of evidence Case series, Level IV.

H. Amano (✉)
Department of Sports Orthopedics, Osaka Rosai Hospital, 1179-3 Nagasone-cho, Kita-ku, Sakai, Osaka 591-8025, Japan
e-mail: h-amano@umin.ac.jp

H. Amano · T. Iwahashi · T. Mae · H. Yoshikawa
Department of Orthopedics, Osaka University Graduate School of Medicine, 2-2 Yamadaoka, Suita, Osaka 565-0871, Japan

T. Suzuki
Department of Orthopedic Surgery, Sapporo Medical University School of Medicine, S1-w16, Chu-ou-ku, Sapporo 060-8543, Japan

N. Nakamura
Faculty of Rehabilitation Science, Osaka Health Science University, 1-9-27, Temma, Kita-ku, Osaka 530-0043, Japan

K. Sugamoto
Locomotor Biomaterial Limited to the Joint Surgery, Osaka University Graduate School of Medicine, 2-2 Yamadaoka, Suita, Osaka 565-0871, Japan

K. Shino
Osaka Yukioka College of Health Science, 1-1-41, Sojiji, Ibaraki, Osaka 567-0801, Japan

K. Nakata
Department of Health and Sport Sciences, Osaka University Graduate School of Medicine, 1-17, Machikaneyama, Toyonaka, Osaka 560-0043, Japan

Keywords Horizontally torn medial meniscus · MRI · 3-D computer model · Movement and deformation

Introduction

Displacement and deformation of the knee meniscus significantly affect its roles in lubrication, shock absorption, load transmission, and laxity of the knee, as well as proprioception in vivo [2, 9, 14, 15, 18]. According to previous studies, a normal meniscus moves posteriorly during knee flexion, and the displacement of the lateral meniscus is larger than that of the medial meniscus [17, 21, 23, 25]. Boxheimer et al. [4] demonstrated that movements of laterally displaceable meniscal tears during knee flexion usually have longitudinal, radial, or complex configurations; however, little is known about the displacement and deformation patterns of a torn medial meniscus.

A quantitative method to analyse kinetics of knee joint using magnetic resonance imaging (MRI) and a three-dimensional (3-D) computer model has been developed [24] and allows for analysis of meniscal displacement and deformation patterns in a torn medial meniscus. Although a horizontal tear of the medial meniscus is not always symptomatic, some patients have knee pain during knee flexion. This method may help to clarify the prognosis and pathology of a horizontally torn medial meniscus, the latter of which is a source of knee pain.

Hypotheses of the present study were as follows: (1) the displacement and deformation of the horizontally torn medial meniscus during knee flexion are correlated with tear size of the 3-D image and (2) when treated conservatively, clinical symptoms of patients with horizontal medial meniscus tears correlate with tear size. The purpose of this study was to evaluate quantitatively the correlations between tear size as revealed by the 3-D image and displacement and deformation of the torn medial meniscus during knee flexion using 3-D MRI and 3-D computer modelling and to compare deformation of horizontal tears with patients' Lysholm scores.

Materials and methods

Twenty patients (14 men, 6 women; mean age, 32.0 ± 11.8 years) with symptoms related to a medial meniscus tear, such as catching, pain with squatting, and recurrent effusions, were included in this study. Four patients had a traumatic episode while performing activities of daily living, and eight had a sport-related traumatic episode; the remaining eight had no episodes. All patients were diagnosed with a horizontal tear in the medial meniscus of Mink's classification type 3 [20] on the basis of two-dimensional MRI. Results of the McMurray's test were positive in eight patients and negative in 12 patients. No degenerative changes were observed in the femorotibial or patellofemoral joint in plain radiographs. Patients received conservative treatment for 3 months, including physical therapy emphasizing the quadriceps muscle, and instructions to refrain from sport activity and squatting. All subjects provided informed consent before study participation.

Acquisition of 3-D MRI

All subjects underwent 3-D MRI in the supine position using a 1.5-Tesla MR scanner (Magnetom Espree, Siemens, Erlangen, Germany) with a circular flexible surface coil (extension position, CP Extremity; Siemens, flexed position, Loop Coil; Siemens). The diameter of the bore (70 cm) provided enough space for 0°–60° knee flexion. True fast imaging with steady-state free precession sequences (fat suppression using the water excitation method; TR, 9.77 ms; TE, 4.33 ms; flip angle, 28°; field of vision, 20 cm; slice thickness, 0.8 mm; matrix, 320 × 256; band width, 300 Hz/pixel; time taken, 6 min) was used to acquire images, as it enabled us to differentiate between cartilage, the meniscus, and water among features within the images [6, 22]. MR images of 15 knees were taken in the four different positions of 0°, 20°, 40°, and 60° of knee flexion and of five knees in the two different positions of 0° and 60°, using a custom-made leg holder with patients in the supine position (Fig. 1). Knee flexion angle was measured using a goniometer. To maintain neutral rotation, the legs were retained in a custom-made leg holder during MR scanning.

3-D model preparation and voxel-based volume registration

The bone, cartilage, and meniscal regions of 3-D MR images were segmented semi-automatically with an intensity threshold segmentation technique using commercially available image analysis software (Virtual Place-M; Medical Imaging Laboratory, Tokyo, Japan). Three-dimensional models of the bone, cartilage, and meniscus were constructed using the marching cubes technique [13] with the Visualization Toolkit (VTK, Kitware, Inc., Clifton Park, NY).

Segmented 3-D MR images of the tibia in the extended position were superimposed over tibial images taken at each position using the voxel-based volume registration method [5], an image processing method for matching voxels in the intersection region between volume images based on voxel values. Correlation coefficients were used to measure similarities in voxel values for registration, minimizing the sum of squared intensity differences for each segmented voxel. Thus, relative positions of the meniscus in relation to the tibia were visualized [7, 16, 24] (Fig. 2a, b, c, d).

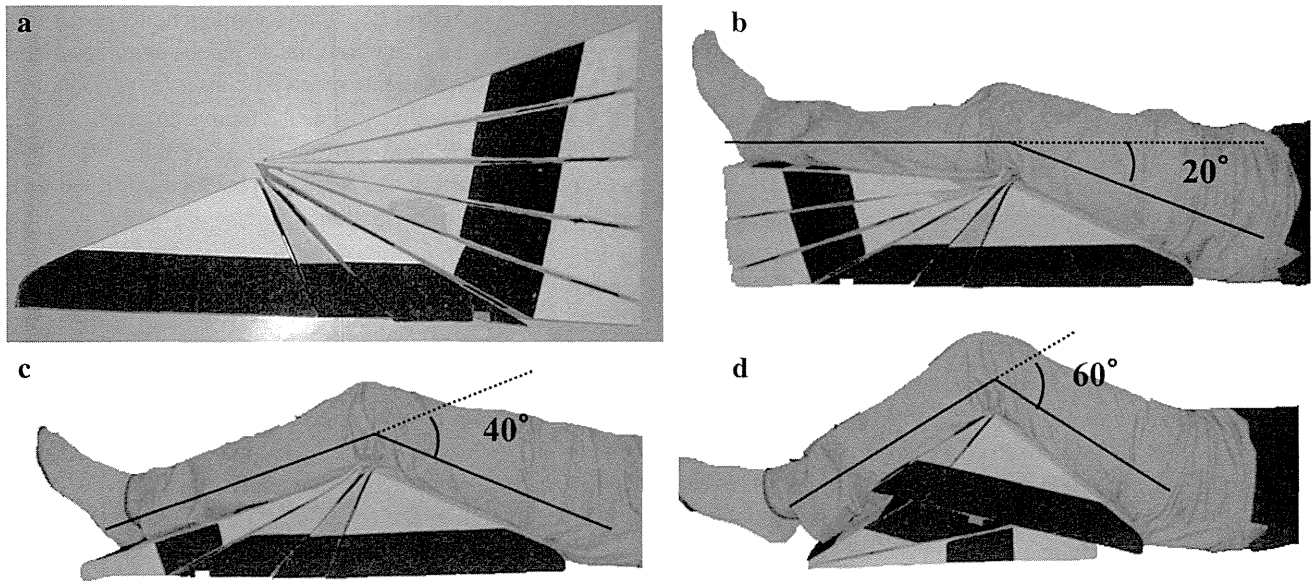

Fig. 1 **a** Image of the custom-made leg holder. The leg holder consists of eight pieces: five 10° pieces, two 20° pieces, and one 90° piece. **b**, **c**, **d** Patient's knee was kept at each angle by combining these pieces

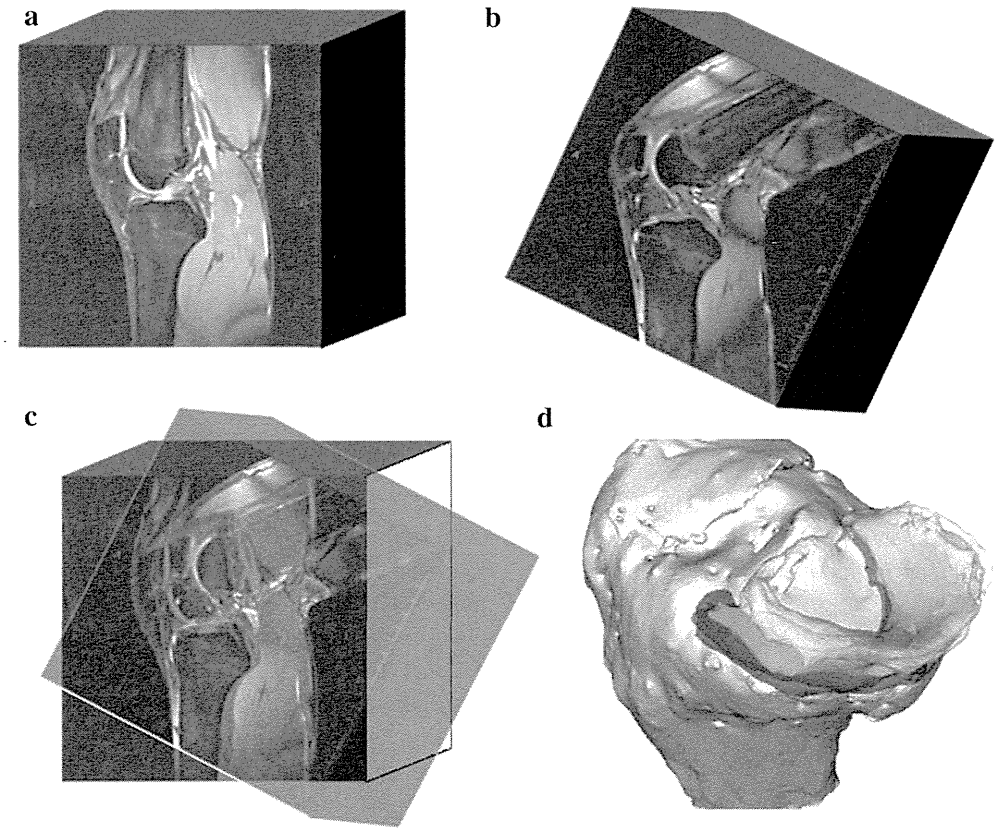

Fig. 2 **a** 3-D MR image in the extended position. **b** 3-D MR image with knee flexion. **c** A 3-D MR image of the tibia in the extended position superimposed over a 3-D MR image of the tibia with knee flexion using the volume registration technique. **d** 3-D computer models of horizontally torn medial menisci at each flexion angle on 3-D computer models of the tibial bone and cartilage in the extended position, visualized by the Visualization Toolkit (VTK, Kitware Inc. Clifton Park, NY)

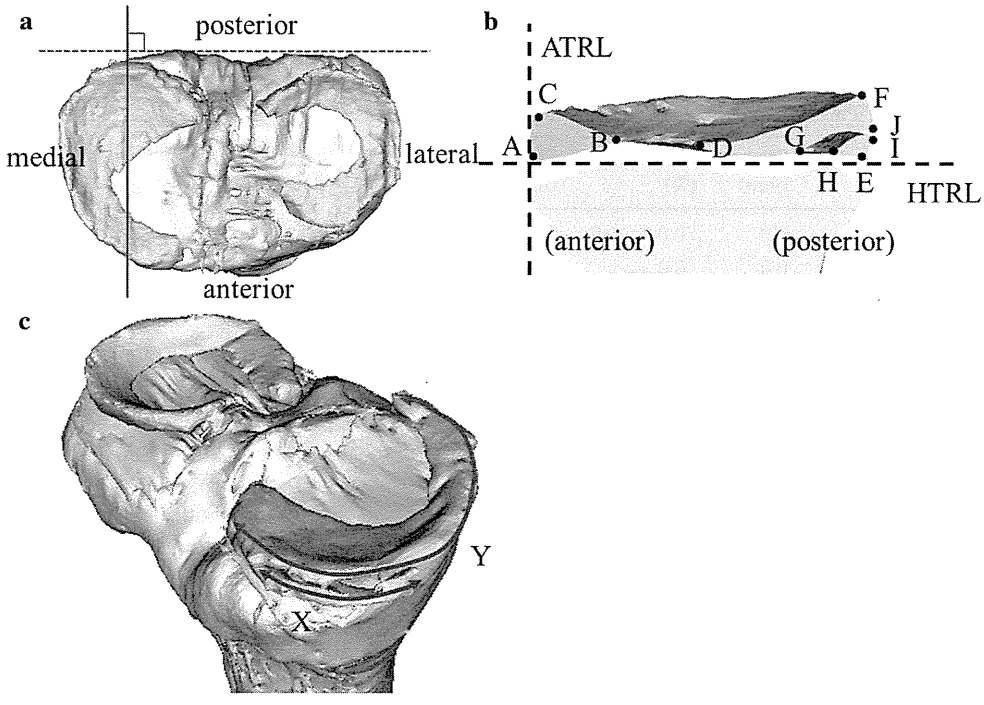

Fig. 3 **a** A 3-D model of the meniscus was cut along the sagittal plane (*red line*), which crossed the most posterior part of the medial tibial plateau. **b** 10 reference points (*black dots*) and two reference lines (*black dashed lines*) were defined. **c** Three-dimensional (3-D) computer models were constructed using the marching cubes technique. The circumferential length of the horizontal tear (*X*, *short double-headed arrow curve*) was measured along the outer rim of the entire circumferential length (*Y*, *long double-headed arrow curve*) of the meniscus on 3-D meniscus models (% tear = *X*/*Y* × 100)

Quantitative evaluation of displacement/deformation and horizontal tear size

Three-dimensional models of the bone and cartilage in the extended position and of the medial meniscus in each position were cut along the sagittal plane through the most posterior point of the meniscus in the extended knee position, which perpendicularly crossed the posterior border of the tibial plateau (Fig. 3a). On the sagittal plane of the bone, cartilage, and medial meniscus, 10 reference points and two reference lines were defined, as described hereafter (Fig. 3b). First, six points (A–F) in the anterior and posterior segments of the medial meniscus were chosen as follows: for the anterior segment, the anteroinferior corner of the cross section of the meniscus (A); the free edge (B); and the anterosuperior corner (C); for the posterior segment, the free edge (D); the posteroinferior corner (E); and posterosuperior corner (F). Second, four points (G–J) were picked in the horizontally torn area: the anterior and posterior margins of the tear on the inferior side (G and H, respectively) and the distal and proximal margins of the tear on the synovial junction (I and J, respectively). Finally, two reference lines were drawn to quantitatively measure the positions of 10 reference points relative to the tibia by employing Shelfelbine [19] and Boxheimer's methods [3]. Briefly, a line paralleling the anterior outermost edge of the articular cartilage of the tibial surface (anterior tibial reference line, ATRL) was set perpendicularly to a line paralleling the cortical surface of the tibial plateau (horizontal tibial reference line, HTRL) on the sagittal plane.

Distances from the reference lines to each point were measured at 0°, 20°, 40°, and 60° of knee flexion in 15 patients and 0° and 60° of knee flexion in five patients. The translation of each point between two different knee flexion angles was calculated from the difference in distance at each knee flexion angle.

The thickness, width, and tear gap of the torn medial meniscus were calculated from the distance between two points. The thickness was determined by the distance between A and C for the anterior segment and between E and F for the posterior segment. The width was determined by the distance between A and B for the anterior segment and between D and E for the posterior segment. The horizontal tear gap was determined by the distance between G and H and the vertical tear gap by the distance between I and J.

To evaluate the size of the horizontal tear, the circumferential ratio of the length of the tear to that of the entire meniscus was calculated on a 3-D computer model of the meniscus in full knee extension, defined as % tear (Fig. 3c). Changes in the tear gap (ΔGH and ΔIJ) between 0° and 60° of knee flexion were calculated, and correlations between ΔGH, ΔIJ, and % tear were evaluated.

Clinical evaluation

The Lysholm score was measured in 15 patients after conservative treatment for 3 months and compared with % tear.

Table 1 Intra-observer and inter-observer standard deviation (SD), coefficients of variation (CV), and intra-class correlation coefficient (ICC) for 20 parameters

Flexion angle	Point	Inter-observer			Intra-observer		
		SD (mm)	CV (%)	ICC	SD (mm)	CV (%)	ICC
0°	A	0.0	0.0	0.9	0.0	0.0	0.9
	B	0.0	0.0		0.6	5.4	
	C	0.6	10.8		0.6	10.2	
	D	1.0	4.4		0.0	0.0	
	E	1.0	2.1		0.6	1.3	
	F	0.6	6.0		0.0	0.0	
	G	1.2	3.4		0.6	1.7	
	H	0.6	1.5		0.6	1.6	
	I	0.6	17.3		0.0	0.0	
	J	0.0	0.0		0.0	0.0	
60°	A	1.5	41.7	0.9	0.0	0.0	0.9
	B	1.2	7.4		0.0	0.0	
	C	0.0	0.0		0.0	0.0	
	D	0.6	2.4		0.6	2.3	
	E	0.6	1.2		0.6	1.2	
	F	1.0	7.7		0.0	0.0	
	G	0.6	1.6		0.6	1.6	
	H	0.6	1.4		0.0	0.0	
	I	0.6	13.3		0.6	15.8	
	J	0.6	7.5		0.6	7.9	

ICCs for inter- and intra-observer were given for flexion angles 0° and 60°, respectively

Reliability measurement

Reliability calculations were based on the positions of 10 points (A–J) measured by the same observer (repeated three times) and by three different observers. The intra- and inter-observer standard deviation (SD), coefficients of variation (CV), and intra-class correlation coefficient (ICC) were calculated. Once the reliability measurements were deemed satisfactory, one of the authors calculated the positions of all 10 points.

The ethical review board of Osaka University approved this study (No. 09157-2).

Statistical analysis

Statistical analysis was performed using SPSS 11.5J (SPSS Japan Inc., Tokyo, Japan). The Wilcoxon signed-rank test was used to compare data at 0° and 60°, including relative positions of A–F, thickness, width, and tear gap of the medial meniscus with a horizontal tear. Spearman's rank correlation coefficient was used to analyse correlations between ΔGH, ΔIJ, and % tear. $p < 0.05$ was considered statistically significant.

Results

Reliability measurement

The intra- and inter-observer SD, CV, and ICC were calculated and are shown in Table 1. All values of ICC exceeded 0.99.

Meniscal displacement and deformation

All menisci examined exhibited backward displacement and deformation during knee flexion, but the pattern of tear gap deformation varied between patients (Fig. 4).

The anteroinferior corner of the anterior segment moved posteriorly during knee flexion ($p < 0.05$), with an increase in the width of the anterior segment ($p < 0.05$), resulting in deformation of the anterior segment. The posteroinferior corner of the posterior segment also moved posteriorly during knee flexion ($p < 0.05$), with an increase in the thickness of the posterior segment ($p < 0.05$), thereby resulting in deformation of the posterior segment. The widths of horizontal and vertical gaps gradually increased with knee flexion ($p < 0.05$) (Table 2).

A direct correlation was observed ($r = 0.68$, $p < 0.05$) between ΔGH and ΔIJ (Fig. 5a).

Horizontal tear size

The size of horizontal tear, defined as % tear, varied between patients and ranged from 13.7 to 55.5 % (mean value, 35.7 ± 12.5 %).

A direct correlation was observed ($r = 0.46$, $p < 0.05$) between % tear and change in the vertical tear gap during 0°–60° knee flexion (ΔIJ) (Fig. 5b). In other words, widening was more significant in a larger tear.

Clinical evaluation

The mean Lysholm score was 80.7 ± 16.4 after conservative treatment. There was an inverse correlation between Lysholm score and % tear ($r = -0.61$, $p < 0.05$) (Fig. 6).

Discussion

The most important finding of the present study was that displacement and deformation patterns in horizontally torn medial menisci were clarified. This study has some advantages over previously reported MR-based kinematic studies on menisci, which evaluated meniscal displacement in cadaveric or normal knees [17, 21, 23, 25]. Boxheimer et al. [4] performed an in vivo kinematic MRI study to characterize a displaceable meniscal tear using vertical

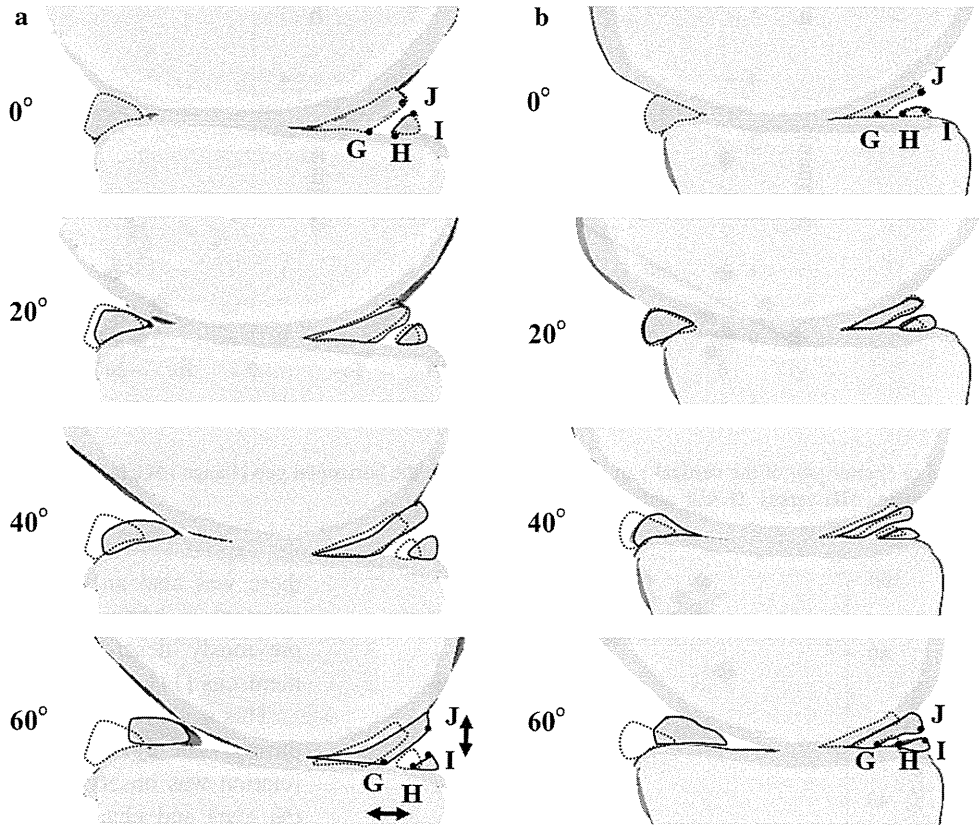

Fig. 4 Deformation of the horizontal tear of the medial meniscus visualized in a 3-D computer model. **a** Case 1. The horizontal gap (GH) and vertical gap (IJ) increased during knee flexion (*black double-headed arrows*). **b** Case 2. The tear gap was barely open during knee flexion

Table 2 Translation of each point and changes in the thickness, width, and tear gap between two knee flexion angles

		Knee flexion			
		0°–20°[b]	20°–40°[b]	40°–60°[b]	0°–60°[c]
Anterior segment	A	0.0 ± 0.0	2.0 ± 0.3	2.8 ± 1.3	4.8 ± 1.5[#]
	B	0.7 ± 1.3	3.0 ± 1.7	4.1 ± 1.3	7.4 ± 2.6[#]
	C	0.2 ± 0.9	3.6 ± 1.4	3.3 ± 1.6	6.6 ± 2.1[#]
	AC[a]	0.3 ± 1.0	−0.5 ± 0.8	0.3 ± 0.8	−0.2 ± 1.1
	AB[a]	0.7 ± 1.3	0.9 ± 1.6	1.3 ± 1.5	2.1 ± 2.2[#]
Posterior segment	D	−0.5 ± 3.1	2.2 ± 2.9	2.8 ± 3.7	4.1 ± 3.6[#]
	E	0.3 ± 2.5	1.7 ± 1.7	2.2 ± 2.3	3.7 ± 2.5[#]
	F	0.6 ± 2.5	1.6 ± 1.7	1.9 ± 2.5	3.7 ± 2.8[#]
	EF[a]	−0.1 ± 1.8	0.9 ± 1.6	1.5 ± 1.6	1.8 ± 1.7[#]
	DE[a]	0.6 ± 1.0	−0.6 ± 1.9	1.3 ± 1.5	−0.4 ± 2.6
Tear gap	GH[a]	0.9 ± 1.3	0.2 ± 1.0	0.5 ± 1.1	1.2 ± 1.7[#c]
	IJ[a]	0.1 ± 1.0	0.9 ± 1.6	1.3 ± 1.5	1.3 ± 1.4[#c]

Values are expressed as mean ± standard deviation (mm)

[#] $p < 0.05$

[a] *AC;* thickness of anterior segment, *AB;* width of anterior segment, *EF;* thickness of posterior segment, *DE;* width of posterior segment, *GH;* horizontal tear gap, *IJ;* vertical tear gap

[b] $n = 15$

[c] $n = 20$

open MRI. In this study, the displacement and deformation patterns of torn menisci were investigated in vivo using 3-D computer models with the volume-based registration technique, which allowed visualization of virtual kinematics and 3-D morphology of a torn medial meniscus [5, 7]. Although some MRI-based studies of the biomechanical

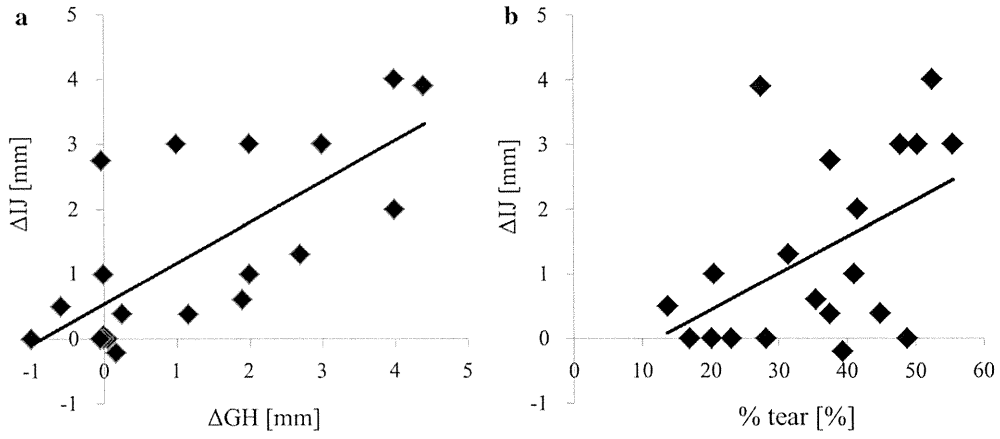

Fig. 5 **a** *Scatter plot* of the vertical gap change (ΔIJ) versus the horizontal gap change (ΔGH) with a best-fit line. **b** *Scatter plot* of the vertical gap change (ΔIJ) versus % tear with a best-fit line

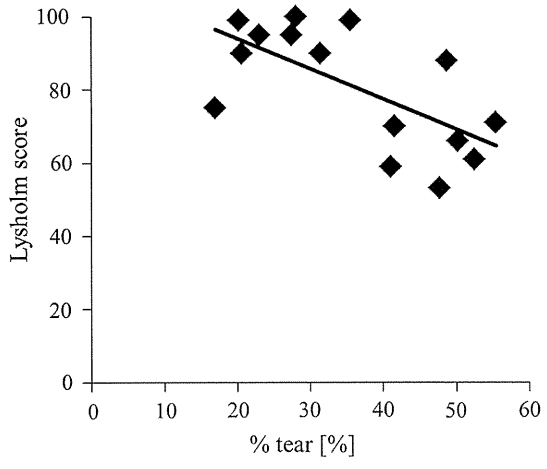

Fig. 6 *Scatter plot* of Lysholm score versus % tear with a best-fit line. $n = 15$

function of the torn meniscus have been reported [1, 10, 12], these studies did not describe the displacement and deformation patterns of torn meniscus as in this study.

Some reports have described the translation of an intact meniscus during knee flexion [21, 23–25]. Yao et al. [25] used MRI to analyse the meniscal translation pattern in normal knees during deep knee flexion and reported that the medial meniscus translated posteriorly by 3.3 mm at the posterior horn and by 6.5 mm at the anterior horn. The results of the present study were similar in that the displacement of a horizontally torn medial meniscus was more pronounced in the anterior segment compared to the posterior segment during knee flexion. Vedi et al. [23] determined changes in meniscal height in normal knees moving from full extension to 90° flexion using a vertical open MR scanner and reported that the height of the posterior horn of the medial meniscus increased by 1.9 mm. In this study, the thickness of the posterior segment increased by 2.1 mm, consistent with Vedi's report. On the other hand, there was also an increase in the width of the posterior segment in horizontally torn medial menisci, unlike the previously described deformation pattern of a normal meniscus [11].

This study showed that the degree of tear gap widening during knee flexion varies among patients. A direct correlation was observed between the size of horizontal tear (% tear) and change in the vertical tear gap (ΔIJ), i.e., larger tear gaps widened more during knee flexion. The inter-individual variation in changes in the tear gap may be associated with differences in the size of the horizontal tear. Although the exact mechanism is unclear, the increase in the tear gap during knee flexion might be caused by the contact of the meniscus with the femoral and tibial cartilage, or due to the strong attachment on the posterior side, which constrains the motion of the medial meniscus. Furthermore, an inverse correlation was observed between tear size and clinical symptoms after conservative treatment for 3 months. These results might explain the pain in patients with horizontally torn menisci, although further studies are warranted.

There were some limitations to this study. First, the accuracy test between an MR image or 3-D computer model of the torn meniscus and the torn meniscus in vivo has not been verified. Although the wedge-shaped, low-signal intensity structure observed on MR images has been shown to accurately represent the normal meniscus in vivo [8], further studies are needed in order to verify the accuracy of a 3-D computer model in representing a torn meniscus in vivo. Second, this study was performed at no more than 60° of knee flexion. Analysis of deep knee flexion over 60° is underway but is limited by pain experienced in patients with horizontal tears. Further investigation is required to obtain more specific details on meniscus displacement and deformation. Third, the present study examined deformation patterns in a non-weight-

bearing position. According to Vedi et al. [23], the translation pattern and changes in meniscal height during knee flexion increased with increasing load, and thus, the displacement and deformation patterns of horizontally torn medial menisci are expected to change with weight-bearing, although further studies are necessary. Finally, there were no controls in this study. The displacement of the intact meniscus has been described previously [17, 21, 23, 25]; therefore, the results of this study were compared to the results described in those reports. Despite these limitations, the meniscal displacement and deformation patterns could be visualized using 3-D computer models reconstructed with 3-D MR images. Understanding the displacement and deformation patterns of a torn medial meniscus may help clarify the cause of pain in patients and facilitate the selection of an appropriate treatment plan.

The clinical relevance of this study is as follows: First, conservative or operative treatment can be selected depending on whether the width of the tear gap increases. Second, this method may help clarify further the pathology for other tear types or assess treatment outcomes via evaluation of functional morphology.

Conclusion

Horizontal tear of the medial meniscus was found to widen and deform posteriorly during knee flexion. Moreover, widening of the tear gap correlated with the size of a horizontal tear, with an inverse correlation between the size of horizontal tear and Lysholm score after conservative treatment.

References

1. Bao HR, Zhu D, Gong H, Gu GS (2013) The effect of complete radial lateral meniscus posterior root tear on the knee contact mechanics: a finite element analysis. J Orthop Sci 18:256–263
2. Bessette GC (1992) The meniscus. Orthopedics 15:35–42
3. Boxheimer L, Lutz AM, Treiber K et al (2004) MR imaging of the knee: position related changes of the menisci in asymptomatic volunteers. Invest Radiol 39:254–263
4. Boxheimer L, Lutz AM, Weishaupt D et al (2006) Characteristic of displaceable and nondisplaceable meniscal tears at kinematic MR imaging of the knee. Radiology 238:221–231
5. Brown LG (1992) A survey of image registration techniques. ACM Comput Surveys 24:325–376
6. Duc SR, Pfirrmann CW, Hodler J et al (2007) Articular cartilage defects detected with 3D water-excitation true FISP: prospective comparison with sequences commonly used for knee imaging. Radiology 245:216–223
7. Goto A, Moritomo H, Ochi T et al (2005) In vivo three-dimensional wrist motion analysis using magnetic resonance imaging and volume-based registration. J Orthop Res 23:750–756
8. Hauger O, Frank LR, Resnick D et al (2000) Characterization of the "Red zone" of knee meniscus: MR imaging and histologic correlation. Radiology 217:193–200
9. Hsieh HH, Walker PS (1976) Stabilizing mechanisms of the loaded and unloaded knee joint. J Bone Jt Surg 58A:87–93
10. Jang KM, Ahn JH, Wang JH (2012) Arthroscopic partial meniscectomy of a posteriorly flipped superior leaflet in a horizontal medial meniscus tear using a posterior transseptal portal. Orthopedics 35:430–433
11. Kawahara Y, Uetani M, Hayashi K et al (1999) MR assessment of movement and morphologic change in the menisci during knee flexion. Acta Radiol 40:610–614
12. Kim YM, Joo YB (2013) Pullout failure strength of the posterior horn of the medial meniscus with root ligament tear. Knee Surg Sports Traumatol Arthrosc 21:1546–1552
13. Lorensen W, Cline H (1987) Marching cubes: a high resolution 3D surface construction algorithm. Comput Graphics 21:163–169
14. Markolf KL, Mensch JS, Amstutz HC (1976) Stiffness and laxity of the knee. The contributions of the supporting structures: a quantitative in vitro study. J Bone Jt Surg 58A:583–594
15. McBride ID, Reid JG (1988) Biomechanical considerations of the menisci of the knee. Can J Sport Sci 13:175–187
16. Moritomo H, Goto A, Yoshikawa H et al (2003) The triquetrum-hamate joint: an anatomic and in vivo three-dimensional kinematic study. J Hand Surg 28A:797–805
17. Scholes C, Houghton ER, Lee M, Lustig S (2013) Meniscal translation during knee flexion: what do we really know? Knee Surg Sports Traumatol Arthrosc. doi:10.1007/s00167-013-2482-3
18. Seedhom BB (1979) Transmission of the load in the knee joint with special reference to the role of the menisci. Part 1: anatomy, analysis and apparatus. Eng Med 8:207–228
19. Shefelbine SJ, Ma CB, Majumdar S et al (2006) MRI analysis of in vivo meniscal and tibiofemoral kinematics in ACL-deficient and normal knees. J Orthop Res 24:1208–1217
20. Stoller DW, Martin C, Mink JH et al (1987) Meniscal tears: pathologic correlation with MR imaging. Radiology 163:731–735
21. Thompson WO, Thaete FL, Fu FH, Dye SF (1991) Tibial meniscal dynamics using three-dimensional reconstruction of magnetic resonance images. Am J Spots Med 19:210–215
22. Vasanawala SS, Hargreaves BA, Gold GE et al (2005) Rapid musculoskeltal MRI with phase-sensitive free precession: comparison with routine knee MRI. Am J Roentgenol 184:1450–1455
23. Vedi V, Williams A, Gedroyc WM et al (1999) Meniscal movement. An in vivo study using dynamic MRI. J Bone Jt Surg 81B:37–41
24. Yamada Y, Toritsuka Y, Shino K et al (2007) Morphological analysis of the femoral trochlea in patients with recurrent dislocation of the patella using three-dimensional computer models. J Bone Jt Surg 89B:746–751
25. Yao J, Lancianese SL, Hovinga KR, Lee J, Lerner AL (2008) Magnetic resonance image analysis of meniscal translation and tibio-menisco-femoral contact in deep knee flexion. J Orthop Res 26:673–684

ELSEVIER

Operative Techniques in
Orthopaedics

Stem Cell Therapy in Cartilage Repair—Culture-Free and Cell Culture–Based Methods

Norimasa Nakamura, MD, PhD,* James Hui, MD, MBBS,† Kota Koizumi, MD,* Yukihiko Yasui, MD,* Takashi Nishii, MD, PhD,* Dnyanesh Lad, MD,‡ Georgios Karnatzikos, MD,‡ and Alberto Gobbi, MD‡

In order to overcome potential problems associated with autologous chondrocyte implantation, mesenchymal stem cell-based therapies could be potential alternatives. Conventional stem cell-based therapy accompanies the separation of cells from tissue followed by monolayer culture for the expansion of cell numbers. On the other hand, the cost of cell culture under quality control is high, which could be a potential barrier for industrialization. In order to reduce the cost associated cell culture, culture-free cell-based therapies have been investigated with the use of bone marrow aspirate. In this chapter, we will introduce the three stem cell-based therapies in cartilage repair. The first two procedures are using cell culture methods and the last one with cell-free method. All the three methods have been into the stage of clinical trials and their surgical procedures as well as their preliminary results will be reported.
Oper Tech Orthop 24:54-60

KEYWORDS stem cell, cartilage repair, cell cuture, knee, clinical trial

Introduction

It is widely accepted that chondral injuries usually do not heal spontaneously.[1,2] Therefore, a variety of approaches have been tested to improve cartilage healing. Among them, chondrocyte-based therapies have been extensively studied since the successful report of autologous chondrocyte implantation. However, this procedure may have limitations including the sacrifice of undamaged cartilage within the same joint and alterations associated with the in vitro expansion of the cells. Furthermore, because of the degenerative changes in cartilage accompanying aging, the availability of the cells may be limited in elderly individuals.[3]

To overcome such potential problems, cell-based therapy using mesenchymal stem cells (MSCs) could be a promising alternative because of the relative ease of harvest and their strong potential for differentiation into multilineage tissues including cartilage.[4,5]

In this article, we introduce 3 interesting topics related to stem cell–based therapy in cartilage repair. The first 2 topics feature the cell culture–based methods (clinical and translational) and the third topic introduces a culture-free method.

This article has been approved by all the institutional review boards and a written informed consent was obtained from every patient before their inclusion in the study.

Bone Marrow MSC–Based Therapy—From Bench to Bedside

There is little doubt among scientific and medical communities that stem cells, especially MSCs, can be used to treat diversified clinical conditions, from immune modulation to tissue

*Department of Orthopaedics, Osaka University Graduate School of Medicine, Osaka, Japan.
†Department of Orthopaedic Surgery, National University of Singapore, Singapore.
‡OASI Bioresearch Foundation, Milan, Italy.
Address reprint requests to Norimasa Nakamura, MD, PhD, Department of Orthopaedics, Osaka University Graduate School of Medicine, Osaka, Japan. E-mail: Norimasa.nakamura@ohsu.ac.jp

 http://dx.doi.org/10.1053/j.oto.2014.02.006
1048-6666/

regeneration. In cartilage repair, there have been many experimental and clinical studies on MSC-based therapy reported with promising results.[6-13] However, unfortunately, the use of stem cells in therapy without proper regulatory and clinical control has been still controversial and, in some way, scandalous.[14-16]

A multidisciplinary orthopaedic-based research group, led by Hui et al, in National University Hospital, Singapore, has systematically developed and translated MSCs for cartilage repair: starting from in vitro research, through animal studies, and finally into clinical trials. First, they have demonstrated that the human bone marrow (BM) is a better source of MSCs than the adipose tissue is.[17] In this study, BM and adipose MSCs were cultured from the same sets of donors. Results showed that although MSCs from both sources were capable of trilineage differentiation, BM MSCs produced significantly more collagen II and s-glycosaminoglycan, suggesting their superior potential for cartilage repair. The next significant progress was demonstrated in small and large animal models, where Lee et al[18] demonstrated that BM MSCs were capable of enhancing cartilage repair.[19]

Nejadnik et al answered an important question of which is superior: autologous BM MSCs vs autologous chondrocyte implantation. In a cohort study, they were able to report comparable efficacy when using BM MSCs as compared with using chondrocytes. The results showed that although both cell types were capable of improving cartilage repair, MSCs were superior in longer-term follow-up, worked just as well in older patients (older than 45 years, which was not replicated in chondrocytes), and required 1 session less of knee surgery, translating into cost savings and potentially lower health risks.[19]

Current techniques of cartilage repair such as autologous chondrocyte implantation require another open surgery after the initial biopsy and harvesting. The use of intra-articular, injectable, cultured, autologous BM MSCs for cartilage repair was investigated and optimized by the research group. Lee et al,[18] using a porcine model, were able to demonstrate the efficacy and viability of using intra-articular injections of MSCs suspended in hyaluronic acid.

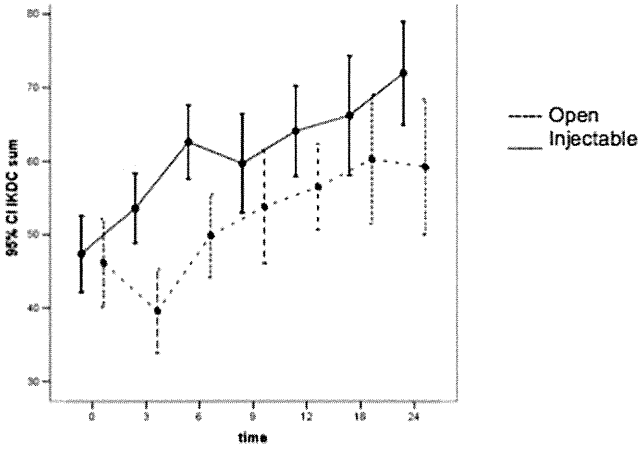

Figure 1 A graph showing the International Knee Documentation Committee (IKDC) sum score: injectable vs open technique.

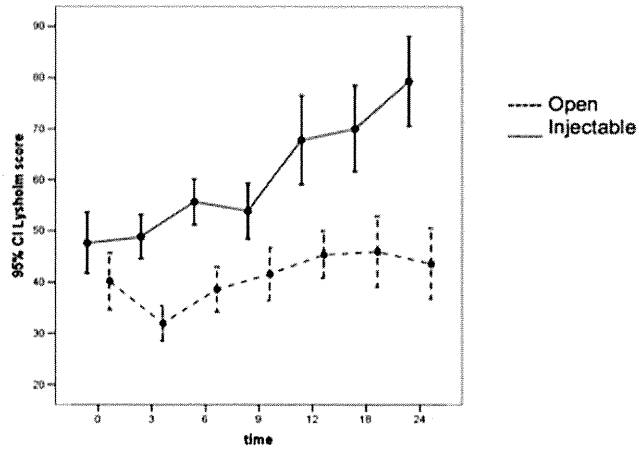

Figure 2 A graph showing the Lysholm score: injectable vs open technique.

In view of concrete consistent evidence from in vitro research to large animal studies, clinical trials are designed and carried out to evaluate the clinical efficacy of using intra-articular, autologous, cultured BM MSCs for cartilage repair. The autologous BM MSCs used are processed in a clean room environment (current good manufacturing practice cell processing facility) and cultured for 3 weeks. From participating subjects, 60 mL of BM and 60 mL of whole blood are collected during the index surgery. The index surgery includes International Cartilage Repair Society classification of the lesion and microfracture techniques as described by Steadman et al.[20,21] After red blood cell removal, the cells are seeded into culture flasks with complete medium change every 2-3 days. When adherent MSCs reach >30% confluency, they are trypsinized and reseeded into the same number of flasks (p0 to p1), usually within 9-12 days. Medium changes continue until MSCs are >80% confluent (usually between 21-28 days after BM collection). Stringent release criteria include no microbial contamination, confluency >80%, normal MSC morphology, and more than 75% viability. The cells are trypsinized and collected, washed, resuspended in autologous serum, and given as intra-articular injections with local anesthesia along with hyaluronic acid.

Clinical trials conducted by Lee et al[22] compared the novel injectable method described earlier with the open technique by which MSCs were implanted beneath a sutured periosteal patch over the defect. In a prospective comparative study comparing both methods with 35 patients in each arm, patients were followed up for 2 years using clinical scoring systems. After 2 years, there were no clinically significant adverse events reported. There was significant improvement in mean International Knee Documentation Committee, Lysholm, SF-36 physical component, and visual analog pain scores in both the groups (Figs. 1 and 2). The injectable group demonstrated better improvement in pain scores and SF-36 scores, but these were statistically insignificant.[22]

Through systematic and careful research and development, MSCs can be safely applied to patients for cartilage repair.

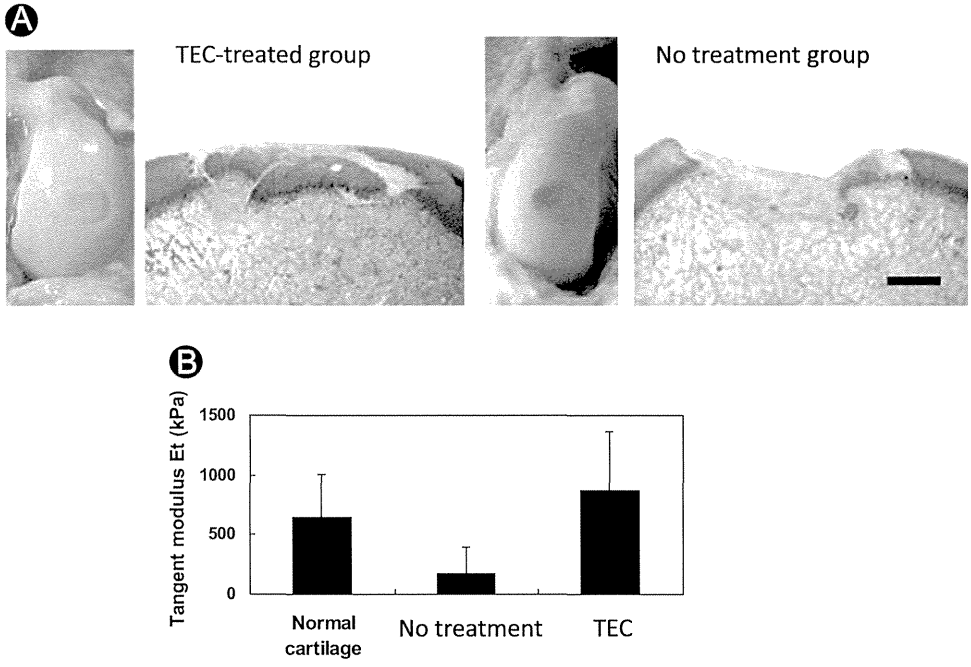

Figure 3 (A) Histology (safranin O staining) of a TEC-treated chondral lesion and an untreated lesion 6 months following implantation in a porcine model. (B) Tangent modules of normal cartilage, of an untreated chondral lesion, and of a TEC-treated chondral lesion at a compression rate of 100 μm/s. There is no significant difference between the value of TEC-treated lesion and that of normal cartilage ($P = 0.297$).

Although clinical results are preliminary, better outcome may be expected when MSCs are added to common surgical procedures. The group's current research work can serve as a model for the development of stem cell therapy into routine applications, but under proper scientific, regulatory, and clinical guidance.

Scaffold-Free Tissue-Engineered Construct Derived From Synovial MSCs

In addition to the selection of cell source, local delivery of cells to chondral lesions is a crucial factor to determine the outcome. It is widely accepted that the appropriate 3-dimensional (3D) environment is important to optimize cell proliferation and chondrogenic differentiation.[23] Therefore, a 3D scaffold, which is seeded with cells, is usually used to repair the defect. Various scaffolds have been approved for clinical use by various governmental institutions.[24] However, there are still several issues associated with the long-term safety of the material. To avoid unknown risk, exogenous materials should ideally be excluded throughout the treatment procedure, and in this regard, a scaffold-free cell delivery system could be a next-generation alternative.[25]

Based on this concept, a scaffold-free, 3D, tissue-engineered construct (TEC) that comprises MSCs derived from synovium and the extracellular matrices synthesized by the cells has been generated.[8,9] The series of in vitro experiments suggest that the TEC may be plastic, adhesive, and capable of chondrogenic differentiation and thus could be feasible to promote cartilage repair. This possibility was confirmed following assessment of TEC implanted in vivo into porcine chondral defects. The TEC firmly attaches to the surface of injured cartilage at the initial stage of implantation, and thus, a sutureless implantation is available. Hereafter, the TEC maintains good tissue integration to the adjacent cartilage matrix, and the repair tissue exhibits chondrogenic differentiation without any evidence of central necrosis up to 6 months after implantation (Fig. 3A). Biomechanical analysis also reveals that the tissue repaired with the TEC implant exhibits modulus similar to the properties of normal cartilage (Fig. 3B). To our knowledge, this study was the first demonstration of a successful MSC-based therapy for the repair of chondral lesions in a clinically relevant injury model without breaching the subchondral plate.[8,9]

Based on the results of the preclinical study, a research group led by Nakamura et al stepped forward to a clinical study at Osaka University Hospital, which has a current good manufacturing practice-grade cell processing center, and submitted the application of the "first-in-men" clinical trial to the Ministry of Health and Labour of Japan in 2011. They got the approval in 2012, and the clinical trial initiated in 2013 after the preparation of good clinical practice-based protocols.[26] The patients with symptomatic chondral lesion of the knee and who meet the inclusion criteria (isolated chondral lesion ≤ 5 cm^2, 20-60 years of age, with normal alignment) have been enrolled in the trail since February 2013. Under general or spinal anesthesia, approximately 1 g of synovial membrane is harvested from the knee joint,

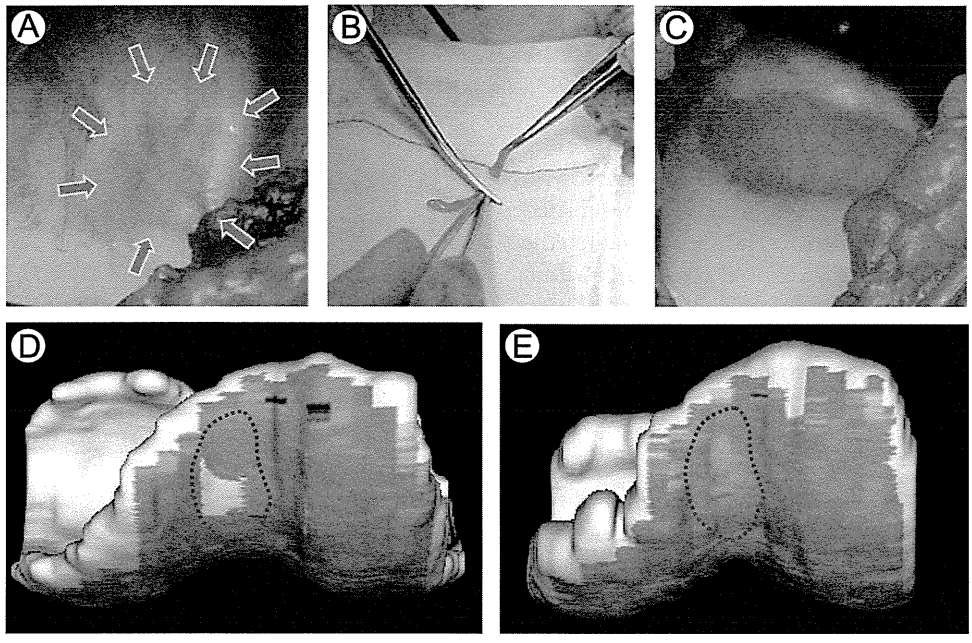

Figure 4 (A) A ICRS Grade III lesion in the medial femoral condyle after debridement. (B) Adjustment of the size of the TEC to match the lesion size just before implantation. (C) Implanted TEC into the lesion. (D) and (E) T2 mapping of the lesion at the femoral groove. (D) Before implantation and (E) 6 months after implantation.

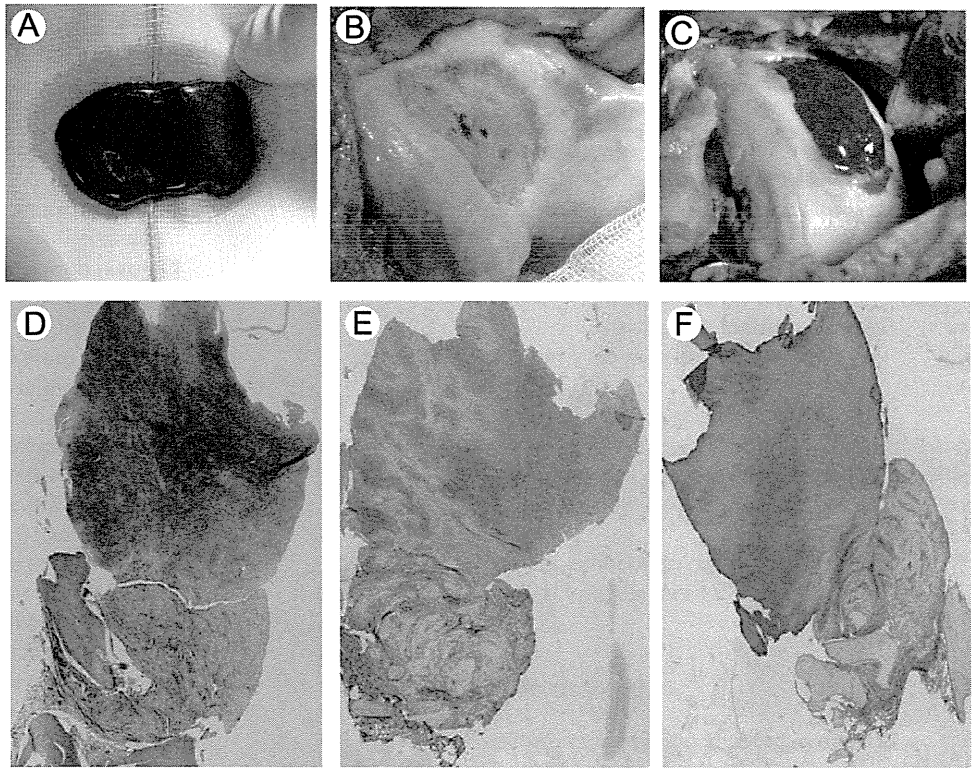

Figure 5 (A) Activated clotlike bone marrow aspirate concentrate (BMAC) after Batroxobin treatment. (B) A Grade IV lesion of the lateral femoral condyle after debridement. (C) Covering of the lesion with a collagen-based matrix, after pasting the clot into the lesion. (D) Biopsy obtained after 24 months. Safranin O staining reveals a well-organized cartilagelike tissue with proteoglycan accumulation. The subchondral bone tissue is in a remodeling process. (E) Findings of the immunohistochemical analysis of collagen type I are almost negative, with only a few Collagen I-positive cells at the superficial layer. (F) Type II collagen is slightly positive in the extracellular matrix and at the cellular level.

which is subject to the culture for the separation and expansion of MSCs. In 3-5 weeks following tissue harvest, the TEC is prepared for implantation. By miniarthrotomy or arthroscopy, the chondral lesion is debrided so as to not breach the subchondral bone (Fig. 4A arrows). Before implantation, the TEC is washed several times with phosphate buffered saline to remove calf serum–related proteins followed by the adjustment of the size to match the chondral defect (Fig. 4B). Implantation is completed within 5-10 minutes, without any reinforcement for fixation (Fig. 4C). After provisional closure of the joint capsule, flexion and extension of the knee is done, followed by the reexposure of the lesion to check the stability of the TEC. The knee is immobilized in a brace for 2 weeks followed by the initiation of range-of-motion exercises and muscle exercises. Full weight bearing is allowed after 6-8 weeks of surgery. Return to strenuous activity is allowed around 12 months following implantation. Based on the type of "first-in-men" study, the duration for follow-up is 1 year and the primary end point of this study is the analysis of adverse reactions. The secondary end point is the assessment of feasibility, which consists of subjective assessment (visual analog score [VAS] for pain [0 = no pain, 10 = worst pain], and knee injury and osteoarthritis outcome score [KOOS]) and structural assessment. For the structural assessment, histologic analysis of the biopsy specimen at 12 months and magnetic resonance imaging (conventional and quantitative such as T2 mapping) at 3, 6, and 12 months are performed (Fig. 4D and E). This clinical study will be completed by March 2015.

Culture-Free Cell-Based Therapy Using Autologous Bone Marrow Aspirate Concentrate

Stem cell–based therapy in cartilage repair has started with the procedure including cell culture process for cell expansion before implantation,[6] which has been followed by many studies.[7-10] Conversely, recent studies have demonstrated that adult stem cells secrete bioactive molecules that stimulate angiogenesis and mitosis of tissue-specific and intrinsic progenitors and reduce T-cell surveillance and inflammation and that mononuclear stem cells are also able to repair damaged tissue.[27-30] These findings suggest that cell selection and cultivation in the laboratory might not be necessary. Here, we describe the techniques and early results of the implantation of culture-free autologous BM aspirate concentrate (BMAC) in chondral lesions. In Orthopaedic Arthroscopic Surgery International Bioresearch Foundation, 25 patients who presented with symptomatic full-thickness chondral lesions of the knee and who met the inclusion criteria (International Centre for Radio Science Grade IV cartilage

Table Rehabilitation Phases and Objectives

Phase	Objectives	Criteria to Progress
Phase 1: protection of implant	Protect the implant from excessive loads and shearing forces	Full active knee extension
	Decrease pain and effusion	Knee flexion $>120^{\circ}$
	Gain full extension and gradual recovery of knee flexion	No pain or minimum pain and swelling
	Retard muscle atrophy	No pain during weight bearing
		Adequate muscle recruitment
Phase 2: recovery of gait	Return to normal gait pattern	Normal gait
	Progressive recovery in daily functional activities	Recovery of nearly full ROM (full extension, flexion $>135^{\circ}$)
	Increase the strength of the quadriceps or flexors	Adequate muscle tone and neuromuscular control
	Recovery of full range of motion	No pain or swelling
Phase 3: maturation and running	Return to a correct running pathway	Running without pain or swelling at 8 kmph for 10 min
	Increase in strength of quadriceps and flexors muscles—further increase in functional activities level	Adequate recovery of coordination and neuromuscular control
		Recovery of strength $>80\%$ Contralateral limb
		Single leg hop test: $>80\%$ contralateral limb
Phase 4: sport-specific recovery	Sustain high loads and impact activities	Running without pain or effusion at 10 kmph for 15 min
	Recovery of sport-specific skills	Recovery of strength $>90\%$ contralateral limb
	Prepare athlete for a return to team and competition with good recovery of the aerobic endurance	Single leg hop test: $>90\%$ contralateral limb
	Maintain a good quality of life, avoiding excess of body fat, and preventing risk of reinjury	Recovery of sport-specific skills

ROM, range of motion.

lesions, 30-60 years of age with body mass index <30, and stable knee with normal alignment or correctable alignment at the time of cartilage repair) were enrolled. They were followed up for a minimum of 3 years. All surgeries were performed by the same surgeon and under spinal anesthesia with routine sterile preparation and draping; 60 mL of BM was harvested from the ipsilateral iliac crest; a sample of which was sent to an independent laboratory to quantify the colony-forming unit (CFU/mL) of MSCs per patient. The BM was centrifuged using a commercially available system following the manufacturer's recommendations so as to concentrate the BM cells 4-6 times. (BMAC Harvest Smart PReP2 System, Harvest Technologies, Plymouth, MA). Using Batroxobin enzyme (Plateltexact, Plateltex S.R.O., Bratislava, SK) the BM concentrate was activated so as to produce a sticky clot material (Fig. 5A). Using a miniarthrotomy, the chondral defect was prepared and debrided so as to obtain a contained, shouldered defect before implantation (Fig. 5B). Specific attention was paid to remove the calcified layer if present, while avoiding penetration of the subchondral bone. Using a template, the collagen membrane was readied and finally, the prepared clot was implanted into the cartilage defect. The collagen-based membrane scaffold (Chondro-Gide, Geistlich Wolhusen, CH) was anchored to the surrounding cartilage using a polydioxanone suture and sealed with fibrin glue (Tissuecol, Baxter. Spa, Rome, Italy) (Fig. 5C). Flexion and extension of the knee were done under arthroscopic visualization to check the stability of the membrane. After surgery, all patients underwent the same rehabilitation program at the same center (Table). Radiographs and magnetic resonance imaging were performed preoperatively at 1 year, 2 years, and final follow-up. Range of motion, VAS for pain (0 = no pain, 10 = worst pain), KOOS, and Tegner and Marx scores were obtained preoperatively and at 12 months, 24 months, and final follow-up. Second-look arthroscopy was performed in 6 knees within 2 years, and 4 patients consented for a concomitant biopsy; the samples were taken from regenerated tissue in the site of the treated chondral lesion and analyzed histologically. All 25 patients (16 males and 9 females) were available at final follow-up (minimum 36 months, average 42 ± 3 months). Analysis of data revealed significant improvement in Tegner and Marx scores, VAS, and KOOS at 1 year, 2 years, and at final follow-up when compared with their respective preoperative scores ($P < 0.05$). All patients returned to previous daily and specific sport activities; however, only 32% were able to perform at the preinjury level at final follow-up.

Second-look arthroscopies revealed a smooth, newly formed tissue that was continuous with the healthy surrounding cartilage. Good histologic findings were reported for the 4 specimens analyzed, which presented with many hyalinelike cartilage features (Fig. 5D-F). Although the biopsy specimens were obtained only from 4 knees, the observed level of maturity, at the latest time point, seems higher than that obtained by other authors with cell suspension autologous chondrocyte transplantation techniques at a similar time point.[31,32]

Use of MSCs in the repair of full-thickness articular cartilage lesions can be a promising treatment option in younger patients who are in need of a salvage procedure. We introduced a culture-free (1 step) method (autologous BMAC). This method can be a viable treatment option for severe chondral lesions of the knee. Longer-term follow-up as well as the future prospective comparative studies are needed to prove the significance of this method as an alternative of autologous chondrocyte implantation.

References

1. Hunter W: On the structure and diseases of articulating cartilage. Philos Trans R Soc Lond B: Biol Sci 9:277, 1743
2. Mankin HJ: The response of articular cartilage to mechanical injury. J Bone Joint Surg Am 64:460-466, 1982
3. Hickery MS, Bayliss MT, Dudhia J, et al: Age-related changes in the response of human articular cartilage to IL-1alpha and transforming growth factor-beta (TGF-beta): Chondrocytes exhibit a diminished sensitivity to TGF-beta. J Biol Chem 278:53063-53071, 2003
4. Gao J, Yao JQ, Caplan AI: Stem cells for tissue engineering of articular cartilage. Proc Inst Mech Eng [H] 221:441-450, 2007
5. Horwitz E, Le BK, Dominici M, et al: Clarification of the nomenclature for MSC: The International Society for Cellular Therapy position statement. Cytotherapy 7:393, 2005
6. Wakitani S, Goto T, Pineda SJ, et al: Mesenchymal cell-based repair of large, full-thickness defects of articular cartilage. J Bone Joint Surg Am 76:579-592, 1994
7. Nakamura T, Sekiya I, Muneta T, et al: Arthroscopic, histological and MRI analyses of cartilage repair after a minimally invasive method of transplantation of allogeneic synovial mesenchymal stromal cells into cartilage defects in pigs. Cytotherapy 14:327-338, 2012
8. Ando W, Tateishi K, Hart DA, et al: Cartilage repair using an in vitro generated scaffold-free tissue-engineered construct derived from porcine synovial mesenchymal stem cells. Biomaterials 28:5462-5470, 2007
9. Shimomura K, Ando W, Tateishi K, et al: The influence of skeletal maturity on allogenic synovial mesenchymal stem cell-based repair of cartilage in a large animal model. Biomaterials 31:8004-8011, 2010; [Epub 2010 Jul 31]
10. Kobayashi T, Ochi M, Yanada S, et al: A novel cell delivery system using magnetically labeled mesenchymal stem cells and an external magnetic device for clinical cartilage repair. Arthroscopy 24:69-76, 2008
11. Wilke MM, Nydam DV, Nixon AJ: Enhanced early chondrogenesis in articular defects following arthroscopic mesenchymal stem cell implantation in an equine model. J Orthop Res 25:913-925, 2007
12. Wakitani S, Okabe T, Horibe S, et al: Safety of autologous bone marrow-derived mesenchymal stem cell transplantation for cartilage repair in 41 patients with 45 joints followed for up to 11 years and 5 months. J Tissue Eng Regen Med 5:146-150, 2011
13. Gobbi A, Karnatzikos G, Scotti C, et al: One-step cartilage repair with bone marrow aspirate concentrated cells and collagen matrix in full-thickness knee cartilage lesions: Results at 2 year follow up. Cartilage 2:286-299, 2011
14. Weissman I: Stem cell therapies could change medicine...if they get the chance. Cell Stem Cell 10:663-665, 2012
15. Cyranoski D: China's stem-cell rules go unheeded. Nature 484:149-150. http://dx.doi.org/10.1038/484149a
16. http://www.chinadailyapac.com/article/beauty-treatment-leaves-4-women-ill-3-critical
17. Afrizah H, Yang Z, Hui JH, et al: A comparison between the chondrogenic potential of human bone marrow stem cells (BMSCs) and adipose-derived stem cells (ADSCs) taken from the same donors. Tissue Eng 13:659-666, 2007
18. Lee KB, Hui JH, Song IC, et al: Injectable mesenchymal stem cell therapy for large cartilage defects—A porcine model. Stem Cells 25:2964-2971, 2007
19. Nejadnik H, Choong PC, Tai BC, et al: Autologous bone marrow-derived mesenchymal stem cells versus autologous chondrocytes implantation: An observed cohort study. Am J Sports Med 38:1110, 2010
20. Brittberg M, Winalski CS: Evaluation of cartilage injuries and repair. J Bone Joint Surg Am 85-A:58-69, 2003

21. Steadman JR, Rodkey WG, Rodrigo JJ: Microfracture: Surgical technique and rehabilitation to treat chondral defects. Clin Orthop Relat Res 391: S362-S369, 2001
22. Lee KB, Wang VT, Chan YH, et al: A novel, minimally-invasive technique of cartilage repair in the human knee using arthroscopic microfracture and injections of mesenchymal stem cells and hyaluronic acid—a prospective comparative study on safety and short-term efficacy. Ann Acad Med Singapore 41:511-517, 2012
23. De Bari C, Dell'Accio F, Luyten FP: Failure of in vitro-differentiated mesenchymal stem cells from the synovial membrane to form ectopic stable cartilage in vivo. Arthritis Rheum 50:142-150, 2004
24. O'Grady JE, Bordon DM: Global regulatory registration requirements for collagen-based combination products: Points to consider. Adv Drug Deliv Rev 55:1699-1721, 2003
25. Huey DJ, Hu JC, Athanasiou KA: Unlike bone, cartilage regeneration remains elusive. Science 338:917-921, 2012
26. https://upload.umin.ac.jp/cgi-open-bin/ctr/ctr.cgi?function=brows&action=brows&type=summary&recptno=R000009672&language=E
27. Fortier LA, Mohammed HO, Lust G, et al: Insulin-like growth factor-I enhances cell-based repair of articular cartilage. J Bone Joint Surg Br 84:276-288, 2002
28. Jones E, McGonagle D: Human bone marrow mesenchymal stem cells in vivo. Rheumatology (Oxford) 47:26-31, 2008
29. Wang L, Li Y, Chen X, et al: MCP-1, MIP-1, IL-8 and ischemic cerebral tissue enhance human bone marrow stromal cell migration in interface culture. Hematology 7:113-117, 2002
30. Caplan AI: Mesenchymal stem cells. The past, the present, the future. Cartilage 1:6-9, 2010
31. Horas U, Pelinkovic D, Herr G, et al: Autologous chondrocyte implantation and osteochondral cylinder transplantation in cartilage repair of the knee joint. A prospective, comparative trial. J Bone Joint Surg Am 85-A:185-192, 2003
32. Knutsen G, Engebretsen L, Ludvigsen TC, et al: Autologous chondrocyte implantation compared with microfracture in the knee. A randomized trial. J Bone Joint Surg Am 86-A:455-464, 2004

J Orthop Sci (2014) 19:925–932
DOI 10.1007/s00776-014-0612-5

ORIGINAL ARTICLE

Patellofemoral chondral status after medial patellofemoral ligament reconstruction using second-look arthroscopy in patients with recurrent patellar dislocation

Keisuke Kita · Yoshinari Tanaka · Yukiyoshi Toritsuka · Yasukazu Yonetani · Takashi Kanamoto · Hiroshi Amano · Norimasa Nakamura · Shuji Horibe

Received: 24 December 2013 / Accepted: 11 July 2014 / Published online: 8 August 2014

Abstract
Background Most patients with recurrent patellar dislocation show cartilage damage in the patellofemoral joint. Medial patellofemoral ligament reconstruction has become one of the most important surgical techniques for treating recurrent patellar dislocation. However, patellofemoral chondral status after this reconstruction has not been elucidated. The purpose of this study was to investigate the effects of medial patellofemoral ligament reconstruction on articular cartilage in the patellofemoral joint by comparing the arthroscopic chondral status at the time of reconstruction with that at second-look arthroscopy.
Methods Participants in the present study comprised 31 patients (22 females, 9 males; 32 knees) who underwent second-look arthroscopy at a median of 12 months (range 6–40 months) after dual tunnel medial patellofemoral ligament reconstruction using a double-looped autologous semitendinosus tendon graft. Median age at the time of initial surgery was 20 years (range 13–43 years). The patellofemoral joint was divided into six portions, comprising the medial facet of the patella, central ridge, lateral facet of the patella, anterior medial femoral condyle, femoral groove, and anterior lateral femoral condyle. Chondral status in each portion according to the International Cartilage Repair Society classification was retrospectively evaluated at the time of initial surgery and second-look arthroscopy.
Results Before medial patellofemoral ligament reconstruction, chondral lesions were observed in the patellofemoral joint in 31 knees (97 %). At the central ridge of the patella, chondral damage was observed in 22 knees (69 %) at initial surgery and damaged cartilages showed recovery in 6 knees. No significant difference in the alteration of chondral status was seen for the medial facet, lateral facet of the patella, anterior medial femoral condyle, femoral groove, and anterior lateral femoral condyle.
Conclusions According to short-term results, the patellofemoral chondral status after medial patellofemoral ligament reconstruction was not altered at second-look arthroscopy in most part of patellofemoral joint. At the

K. Kita (✉) · Y. Tanaka · T. Kanamoto · H. Amano
Department of Sports Orthopaedics, Osaka Rosai Hospital, 1179-3 Nagasone-cho, Kita-ku, Sakai, Osaka 591-8025, Japan
e-mail: keikita@hera.eonet.ne.jp

Y. Tanaka
e-mail: yoshi-tanaka@orh.go.jp

T. Kanamoto
e-mail: takanamoto2@gmail.com

H. Amano
e-mail: h-amano@umin.ac.jp

Y. Toritsuka
Department of Sports Orthopaedics, Kansai Rosai hospital, 3-1-69 Inabaso, Amagasaki, Hyogo 660-8511, Japan
e-mail: toritsuka@kanrou.net

Y. Yonetani
Department of Orthopaedic Surgery, Osaka University Graduate School of Medicine, 2-2 Yamadaoka, Suita, Osaka 565-0871, Japan
e-mail: yonechanosk@gmail.com

N. Nakamura
Department of Rehabilitation Science, Osaka Health Science University, 1-9-27 Tenma, Kita-ku, Osaka, Osaka 530-0043, Japan
e-mail: viader7jp@yahoo.co.jp

S. Horibe
Faculty of Comprehensive Rehabilitation, Osaka Prefecture University, 3-7-30 Habikino, Habikino, Osaka 583-8555, Japan
e-mail: s-horibe@rehab.osakafu-u.ac.jp

central ridge of the patella, significant improvement of the International Cartilage Repair Society grading was observed.

Introduction

The importance of the medial patellofemoral ligament (MPFL) as the primary soft-tissue restraint to lateral displacement of the patella has been corroborated by several studies [1–3], and MPFL reconstruction has become one of the most important surgical techniques for treating recurrent patellar dislocation [4, 5]. Many operative techniques to reconstruct the MPFL have been described, and good mid-term clinical results with up to 97 % patient satisfaction and over 10 years of follow-up have been reported [6].

Most patients with recurrent lateral patellar dislocation show cartilage damage in the patellofemoral joint caused by excessive lateral load, and continuation of patellar dislocation exacerbates patellar cartilage lesions [7]. Several in vitro studies have shown good effects of MPFL reconstruction on patellofemoral kinematics and contact pressure [8, 9]. Articular cartilage lacks a blood supply and is thus regarded as having poor healing potential [10]. However, one report supports the notion that cartilage lesions caused by abnormal knee kinematics may be healed with the restoration of normal knee kinematics [11]. This fact may be relevant to MPFL reconstruction.

On the other hand, over-tensioning of the graft and non-anatomical surgery reportedly have adverse effects on patellofemoral articular cartilage. Moreover, the usage of a much stronger tendon than the native MPFL, such as the semitendinosus tendon or gracilis tendon, could also adversely affect the patellofemoral joint [12]. MPFL reconstruction thus still carries a risk for the development of osteoarthritis, and clarification is needed to show whether the restoration of normal patellar tracking and preventing further dislocation by MPFL reconstruction can change the natural course of cartilage damage in patients with recurrent patellar dislocation and avert further development of osteoarthritis.

One study has investigated the arthroscopic chondral status after MPFL reconstruction [13]. However, the detailed location-specific response of damaged articular cartilage after MPFL reconstruction has not been described. The purpose of this study was to compare arthroscopic chondral status at MPFL reconstruction with that at second-look arthroscopy and to investigate the effects of MPFL reconstruction on the articular surface of the patellofemoral joint. Our hypothesis was that anatomical MPFL reconstruction would not aggravate the patellofemoral joint surface.

Materials and methods

Patients

Between 2000 and 2009, a total of 81 patients underwent MPFL reconstruction using double-looped semitendinosus tendon at our hospital. All patients had patellar dislocation twice or more and had been diagnosed with recurrent patellar dislocation on physical examinations, showing a positive apprehension sign in all cases. Among all 81 patients, 8 with a history of prior knee surgery (osteochondral fracture fixation, 3 patients; medial tubercle transfer, 2 patients; lateral retinaculum release, 2 patients; medial reefing, 1 patient) and 2 (2.5 %) who had suffered postoperative patellar fractures were excluded from the investigation. One patient (1.2 %) with re-dislocation during the follow-up period was also excluded from the study. All patients included in this study underwent only MPFL reconstruction using double-looped semitendinosus tendon without any other additional surgical procedure or any intervention involving articular cartilage. Prior to MPFL reconstruction, informed consent for second-look arthroscopy 1-year after the initial surgery was obtained from all patients. Participants in the present study comprised 31 patients (22 females, 9 males; 32 knees) who underwent second-look arthroscopy at a median of 12 months postoperatively (range 6–40 months) with 2 or more years of follow-up. Median age at the time of MPFL reconstruction was 20 years (range 13–43 years). Median Tegner activity score was 4 (range 3–9) (Table 1). According to Wiberg's classification, the shape of the patellae of 12 patients was classified as type II and that of 20 patients was as type III. Based on trochlear dysplasia classification according to Dejour [14], 7 knees had type A trochlear dysplasia, 2 had type B, 8 had type C, and 12 had type D. The study was approved by the local ethics committee and was conducted according to the principles of the Declaration of Helsinki. The patients were informed that data from the case would be submitted for publication and gave their consent.

Surgical technique

All reconstructions were performed using a modified "dual tunnel medial patellofemoral ligament reconstruction" technique, as reported by Toritsuka et al. [15]. First, chondral status and patellar tracking were carefully evaluated by arthroscopy. A semitendinosus autograft was then harvested. The distal end of the tendon was used and doubled over. A small 1-cm incision was made on the lateral side of the patella, and a skin incision approximately 5 cm in length was made from the medial patellar edge to the medial femoral epicondyle. Two patellar guidewires

Table 1 Demographic data and arthroscopic findings

Patient	Sex	Age	Tegner activity scale	Wiberg classification	Dejour's trochlear dysplasia classification	ICRS classification											
						Before MPFL reconstruction						Second-look arthroscopy					
						MP	CR	LP	MF	FG	LF	MP	CR	LP	MF	FG	LF
1	M	23	4	3	C	0	4	4	0	0	0	0	2	2	0	0	0
2	F	31	3	3	D	0	2	0	0	4	0	0	2	0	0	4	0
3	F	15	4	2	C	4	2	2	0	0	1	4	2	2	0	0	0
4	F	16	9	3	D	3	4	0	0	0	0	3	3	0	0	1	0
5	M	20	8	3	D	0	4	0	0	0	2	0	4	0	0	2	0
6	F	14	4	3	D	0	3	0	0	2	0	0	3	0	0	2	0
7	F	33	3	3	C	0	4	0	0	0	0	0	4	0	0	0	0
8	M	27	6	3	A	2	0	0	0	0	0	3	0	0	0	1	0
9	F	20	3	3	D	0	4	0	0	1	0	0	4	0	0	1	0
10	F	18	4	3	B	0	1	0	0	0	1	0	1	0	0	0	0
11	M	18	9	2	D	0	4	0	0	0	2	0	4	0	0	0	2
12	M	28	4	3	D	4	0	0	0	0	1	4	0	0	0	0	0
13	M	20	7	3	B	4	2	0	0	2	0	4	2	0	0	2	0
14	M	23	6	2	A	3	0	0	0	0	0	3	0	0	1	0	0
15	M	18	9	2	C	0	3	0	0	0	0	0	3	0	0	0	0
16	F	16	4	3	C	0	4	0	0	0	0	0	2	0	0	0	0
17	F	28	3	2	C	0	2	0	1	0	0	0	2	0	0	0	0
18	F	21	3	3	D	3	0	0	0	0	2	3	0	0	0	0	2
19	F	18	3	2	A	0	4	0	0	0	0	0	3	0	0	0	0
20	F	14	7	3	D	0	1	0	0	0	0	0	1	0	0	1	0
21	F	39	7	2	C	0	2	0	0	0	2	0	2	0	0	0	1
22	F	20	4	3	A	0	2	0	0	0	3	0	1	0	0	0	0
23	F	13	7	2	A	0	1	0	0	0	0	0	1	0	0	0	0
24	F	17	3	3	D	2	0	0	0	0	0	2	0	0	0	0	0
25	F	22	3	3	N	0	0	1	0	0	0	0	0	1	0	0	0
26	F	13	3	3	N	0	4	0	0	0	0	0	2	0	0	0	0
27	F	39	3	2	D	1	0	0	0	0	0	2	0	0	0	0	0
28	M	14	7	3	N	3	0	0	0	0	0	3	0	0	0	0	0
29	F	43	6	3	A	4	0	0	2	0	0	1	0	0	1	0	0
30	F	23	3	2	C	0	2	0	0	0	0	0	2	0	0	0	0
31	F	35	3	2	A	0	2	0	0	0	0	0	2	0	0	1	0
32	M	17	3	2	D	2	0	0	0	0	0	2	0	0	0	1	0

MP medial facet of the patella, *CR* central ridge of the patella, *LP* lateral facet of the patella, *MF* anterior medial femoral condyle, *FG* femoral groove, *LF* anterior lateral femoral condyle, *N* normal

were transversely inserted, one from the proximal one third of the medial edge of the patella and the other from the center of the patella. Patellar guidewires were over-drilled using a 4.5-mm cannulated reamer to create sockets with a depth of 15 mm. Another guidewire was inserted from the superoposterior portion of the medial femoral epicondyle toward the proximal cortex of the lateral femoral condyle. The guidewire was overdrilled with an ENDOBUTTON® drill (Smith and Nephew Endoscopy, Andover, MA), and a 5–6 mm socket was created at the anatomical femoral insertion of the MPFL. The center of the graft was pulled into the femoral socket and fixed using an ENDOBUTTON®. The two free ends of the graft were pulled into the bone sockets of the patella and fixed using an ENDOBUTTON® on the lateral side of the patella at 45° of knee flexion. At this time, care was taken not to place too much tension on the graft. After fixation of both sites, negative manual lateral dislocation of the patella was confirmed.

Postoperative Management

The knee was immobilized with a brace at 45° of knee flexion. Upon removal of the brace at 2 weeks after MPFL reconstruction, passive and active-assisted range of motion exercises for the knee were started. Weight-bearing was gradually increased to full at 4 weeks postoperatively. Running was allowed at 3 months, followed by a return to previous sporting activity at 6 months [13].

Evaluations

Chondral status of the patellofemoral joint according to the International Cartilage Repair Society (ICRS) classification [16] was retrospectively evaluated using photographs taken both at the time of MPFL reconstruction and at the second-look arthroscopy through lateral suprapatellar and anterolateral parapatellar portals. The photographs taken both at the initial surgery and at the second second-look arthroscopy were evaluated by the senior author and the corresponding author, respectively. The patellofemoral joint was divided into six portions, comprising the medial facet, central ridge and lateral facet of the patella, and the anterior medial femoral condyle, femoral groove, and anterior lateral femoral condyle. Chondral status in each portion at the time of MPFL reconstruction was compared with that at second-look arthroscopy. Clinical data including the incidence of recurrent patellar subluxation or dislocation, lateral patellar mobility, lateral patellar apprehension sign, and Kujala score were evaluated. Pre- and postoperative radiographic values including the sulcus angle, lateral tilt angle, and congruence angle were also evaluated [13].

Statistical analysis

The data analyses were expressed as mean ± standard deviation (SD) of the mean. Statistical analyses were performed using Student's t test and the Wilcoxon rank-sum test. Values of $P < 0.05$ were defined as significant.

Results

All patients showed a normal range of motion at the time of second-look arthroscopy. As for passive patellar mobility, abnormal lateral patellar movement was identified in all cases preoperatively. At second-look arthroscopy, all patellae were firmly fixed within the femoral groove, and no abnormal lateral mobility was evident in any case. Mean Kujala score improved from 72 ± 8 to 94 ± 5 at 2-year follow-up. While 28 knees showed clear improvements in the apprehension sign, positive results were still evident in 4 knees. Mean sulcus angle was 147.8° ± 8.9°.

Table 2 Radiographic measurement

	Before MPFL reconstruction	Immediately after MPFL reconstruction	Second-look arthroscopy
Lateral tilt angle (°)	−6.1 ± 15.6	5.4 ± 9.3[a]	−2.6 ± 13.8[a,b]
Congruence angle (°)	17.4 ± 22.8	−11.3 ± 18.7[a]	7.8 ± 22.3[a,b]

Values are expressed as mean ± standard deviation

[a] $P < .05$ compared with before MPFL reconstruction

[b] $P < .05$ compared with immediately after MPFL reconstruction

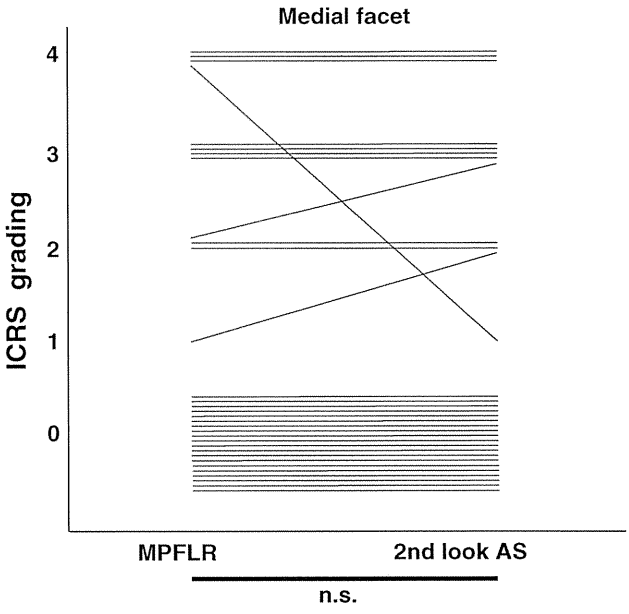

Fig. 1 Chondral status of the medial facet of the patella according to ICRS grading at MPFL reconstruction and at second-look arthroscopy

Preoperatively, mean lateral tilt angle and mean congruence angle were −6.1° ± 15.6° and 17.4° ± 22.8°, respectively. Immediately after MPFL reconstruction, these indices had improved. At second-look arthroscopy, these indices had returned toward preoperative values to some extent (Table 2). However, significant improvement was still seen at second-look arthroscopy.

At the time of MPFL reconstruction, chondral lesions were observed in the patellofemoral joint in 31 cases (97 %). Chondral damage at the medial facet of the patella was observed in 12 knees at MPFL reconstruction. No change of ICRS grading was observed in nine knees. One knee improved from grade 4 to 1. Two knees deteriorated (one knee from 2 to 3, one knee from 1 to 2). No significant difference in alteration of chondral status was seen for this location (Fig. 1). At the central ridge of the patella, chondral damage was observed in 22 knees at initial surgery. Of these, six knees exhibited improvement of ICRS grading (two knees from 4 to 3, three knees from 4 to 2,